SOFT ROBOTICS
Volume 00, Number 00, 2023

DOI: 10.1089/soro.2023.0022

SoRo
Soft Robotics

Open camera or QR reader and scan code to access this article and other resources online.

A Dual-Modal Hybrid Gripper with Wide Tunable Contact Stiffness Range and High Compliance for Adaptive and Wide-Range Grasping Objects with Diverse Fragilities

Jiaqi Zhu,[1,2] Han Chen,[1] Zhiping Chai,[1] Han Ding,[1] and Zhigang Wu[1]

Abstract

The difficulties of traditional rigid/soft grippers in meeting the increasing performance expectations (e.g., high grasping adaptability and wide graspable objects range) of a single robotic gripper have given birth to numerous soft–rigid coupling grippers with promising performance. However, it is still hard for these hybrid grippers to adaptively grasp various objects with diverse fragilities intact, such as incense ash and orange, due to their limited contact stiffness adjustable range and compliance. To solve these challenging issues, herein, we propose a dual-modal hybrid gripper, whose fingers contain a detachable elastomer-coated flexible sheet that is restrained by a moving frame as a teardrop shape. The gripper's two modes switched by controlling the moving frame position can selectively highlight the low contact stiffness and excellent compliance of the teardrop-shaped flexible sheets and the high contact stiffness of the moving frames. Moreover, the contact stiffness of the teardrop-shaped sheets can be wide-range adjusted by online controlling the moving frame position and offline replacing the sheets with different thicknesses. The compliance of the teardrop-shaped sheets also proves to be excellent compared with an Ecoflex 10 fingertip with the same profile. Such a gripper with wide-range tunable contact stiffness and high compliance demonstrates excellent grasping adaptability (e.g., it can safely grasp several fragile strawberries with a maximum size difference of 18 mm, a strawberry with a left/right offset of 3 cm, and a strawberry in two different lying poses) and wide-range graspable objects (from 0.1 g super fragile cigarette ashes to 5.1 kg dumbbell).

Keywords: robotic gripper, multiple modes, soft–rigid design, grasping adaptability, wide-range grasping

Introduction

Grasping is an essential operation in numerous scenarios, such as human–robot interaction,[1–4] biological sample collection,[5,6] and food processing.[7–10] A single robotic gripper with high grasping performance including high grasping adaptability (the capability of grasping a specified object with random size, offset, and pose with the same input) and wide-range graspable objects has long been desired. Traditional rigid grippers can manipulate various rigid and

[1]Soft Intelligence Laboratory, State Key Laboratory of Digital Manufacturing Equipment and Technology, Huazhong University of Science and Technology, Wuhan, China.
[2]Department of Mechanical and Automation Engineering, The Chinese University of Hong Kong, Hong Kong SAR, China.

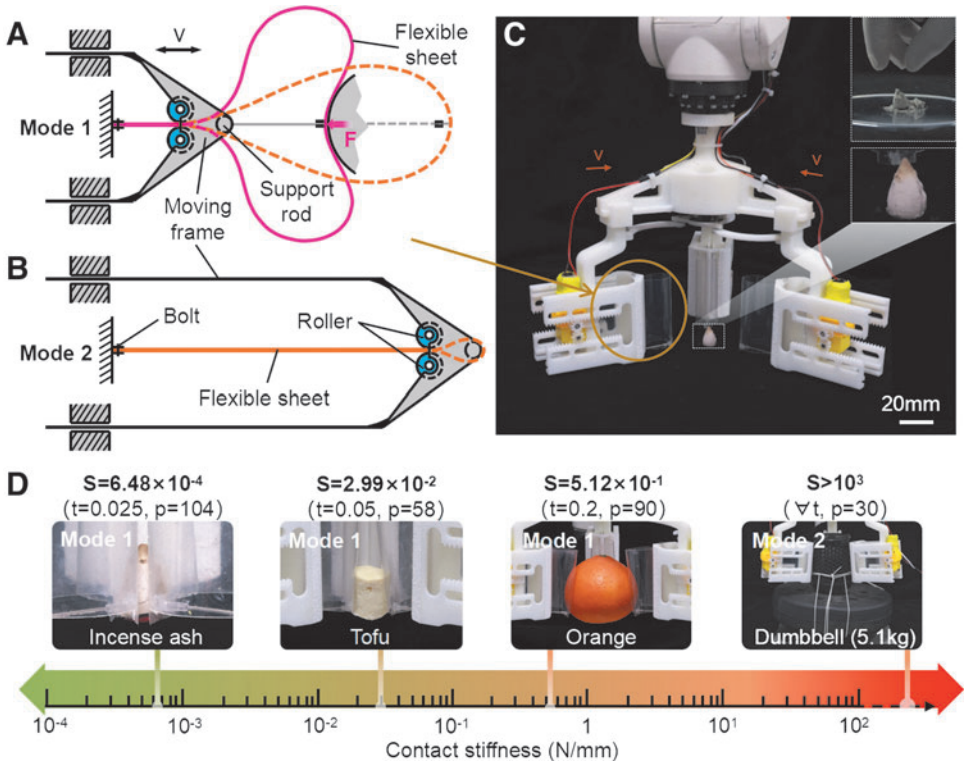

FIG. 1. Dual-mode hybrid gripper. **(A)** Schematic diagram of the hybrid gripper's finger in Mode 1. **(B)** Schematic diagram of the hybrid gripper's finger in Mode 2. **(C)** Physical photograph of the hybrid gripper. **(D)** The contact stiffness of the dual-mode hybrid gripper can vary across several orders of magnitude, allowing it to safely grasp a wide range of objects from fragile and lightweight objects, such as incense ash and tofu, to heavy and rigid objects such as dumbbells. The t means thickness and the p means perimeter.

heavy objects due to their high output force, but their high contact stiffness and low compliance greatly increase their difficulty in grasping fragile objects and decrease their grasping adaptability.[11–15]

Conversely, soft grippers, mainly made of soft materials, exhibit good grasping adaptability and have inherent advantages in manipulating fragile objects.[16–23] However, their low structural stiffness and output force greatly limit their load capacity. Although the introduction of various variable stiffness mechanisms, such as granular jamming,[24–28] low-melting point alloys,[29] and shape memory materials,[19,30–33] can improve their load capacity to some extent, the gaps between the load capacity of soft grippers and that of the rigid grippers are still quite large.

In addition, for most soft grippers, safely grasping some extremely fragile objects, for example, incense ash, remains difficult, as their contact stiffness adjustable range is usually quite limited and it is hard for them to achieve a quite low contact stiffness without sacrificing their limited load capacity. Also, their compliance, usually provided by their soft fabrication materials, still needs to be further improved.

Soft–rigid coupling design methods, targeting to share the respective advantages of soft and rigid structures in a compact robotic system, might be an ideal way to solve the aforementioned problems.[34–38] Up to now, a series of soft–rigid coupling (hybrid) grippers with promising performance have been proposed.[39–43] For example, a bioinspired two-fingered hybrid gripper with multiple modes and poses can grasp wide-range objects from 0.1 g potato chips to a 27 kg dumbbell.[39] For these hybrid grippers, an effective soft–rigid collaboration strategy is usually necessary to help them realize the complementarity between soft and rigid structures.

Although the grippers' grasping adaptability and graspable object range can be significantly enhanced by introducing soft–rigid coupling design methods, it is still quite hard for most existing hybrid grippers to adaptively grasp various objects with diverse fragilities intact, such as incense ash, tofu, and orange, as their soft structures still suffer from inadequate contact stiffness adjustable range and limited compliance.

To solve the aforementioned problems, herein, we propose a dual-modal hybrid gripper with three hybrid fingers that can flexibly switch between two functional modes by actively extending or retracting rigid structures (Fig. 1). The hybrid finger of the gripper is mainly composed of a detachable elastomer-coated flexible sheet and a rigid moving frame that restrains the outer sheet as a teardrop shape from a top–down view. With the movement of the moving frame, the low contact stiffness and excellent compliance of the teardrop-shaped flexible sheet and the high contact stiffness of the moving frame can be selectively highlighted (Fig. 1A–C).

Moreover, the contact stiffness of the teardrop-shaped sheet can be adjusted in a wide range by online adjusting the moving frame position or offline replacing various sheets with different thicknesses, so as to adapt to objects with diverse degrees of fragility. Such a teardrop-shaped sheet also proved to have better contact compliance than a common soft fingertip made of Ecoflex 10 (the softest material among commonly used materials in soft robots) with the same profile.

We introduced the gripper's design and implementation, systematically studied the contact stiffness and contact compliance of its fingers in Mode 1 (the mode in which the teardrop-shaped flexible sheets are exposed), and finally demonstrated its grasping performance (i.e., grasping adaptability and graspable object kinds and range) by using it to grasp a series of fragile strawberries with different sizes, offsets, and poses, and various objects with diverse fragilities (Fig. 1D).

Design and Implementation

Working principle

As shown in Figure 1A, the finger of our gripper mainly consists of a detachable flexible sheet and a rigid moving frame. The moving frame can restrain the flexible sheet through its two rollers to make the outer sheet a teardrop shape. If we press an object with the tip of such a teardrop-shaped sheet, the flexible sheet will deform compliantly and generate corresponding press force. By controlling the position of the moving frame, the soft and rigid parts of the finger can be selectively highlighted, forming the following two modes for different scenarios:

1. When the gripper needs to grasp some lightweight and fragile objects, for example, incense ash and origami paper cranes, the moving frame can retract and expose the teardrop-shaped flexible sheet, which has relatively low contact stiffness and will deform compliantly and apply gentle press force upon contacting with the target objects, as shown in Figure 1A.
2. When the gripper needs to grasp some rigid and heavy objects, for example, dumbbells, the moving frame can move forward to make its support rod against the teardrop-shaped flexible sheet. At this point, the finger is equivalent to an ordinary rigid finger with high contact stiffness, as shown in Figure 1B.

Several of such fingers can be assembled on a base to form a gripper that can grasp various objects by controlling the opening and closing of the fingers, as shown in Figure 1C. A kinematic model and a static model of the gripper have been established, respectively, in Section S1 of the Supplementary Data and Supplementary Figure S1 to facilitate the motion control and maximum output force evaluation of its fingers.

In Mode 1, since the contact stiffness of the teardrop-shaped flexible sheet varies with its geometric parameters, a relevant static model was established in Section S2 of the Supplementary Data and Supplementary Figure S2 to study the intrinsic relationship. The theoretical model analysis indicates that the contact stiffness of the teardrop-shaped flexible sheet is proportional to the cube of its thickness and inversely proportional to the cube of its perimeter. Therefore, we can tune the finger's contact stiffness in Mode 1 by adjusting the two parameters of the teardrop-shaped flexible sheet.

The perimeter can be continuously online adjusted by controlling the position of the moving frame, whereas the thickness can be quickly offline adjusted by conveniently replacing the flexible sheet (the detailed replacement process of the flexible sheet is shown in Supplementary Movie S1). The cubic relationships can endow the finger in Mode 1 with a wide-range tunable contact stiffness, which facilitates its grasping of various objects with diverse fragilities, and thus greatly enhances the gripper's versatility, as shown in Figure 1D.

It should be noted that the size change of the teardrop-shaped flexible sheet caused by the position change of the moving frame will lead to a slight forward/backward movement of the contact point (also the tipping point of the teardrop-shaped flexible sheet) between the finger and the objects. To study the position change of the contact point, a theoretical model was built and the corresponding verification tests were conducted in Section S3 of the Supplementary Data and Supplementary Figure S3. The results show that there is a linear relationship between the contact point position and the moving frame position, and the change ratio of the two is as low as 0.169.

Structural design

As shown in Figure 2 and Supplementary Figure S4, the gripper consists of three circumferentially distributed fingers with a soft–rigid coupling structure. Each finger contains a flexible sheet whose two ends are fixed by a pair of splints through bolting. The splints are further installed on the moving base. A moving frame is fitted to the sliding rails of the moving base and can move along them. A dual-axis DC motor is used to stably control the movement of the moving frame with the help of two pairs of meshing gears (each pair includes one driving gear and one driven gear).

A pair of rollers with a ripple-shaped outer surface is installed on the moving frame to restrain the deformation of the flexible sheet with low friction. To prevent the outer teardrop-shaped flexible sheet from tipping over, a guide rod is fitted to the silicone tube glued on the flexible sheet. Moreover, to increase the friction between the finger and the objects, frosted nonslip tapes can be stuck to the outer surfaces of the moving frame, as shown in Supplementary Figure S5. Such fingers can fit the sliding rails of the fixed base through their chutes on the moving bases, and their movement can be controlled by the curved pull rods connected with a steering engine.

In practice, there is a trade-off relationship between the diameter of the support rod and the perimeter range of the teardrop-shaped flexible sheet. As shown in Supplementary

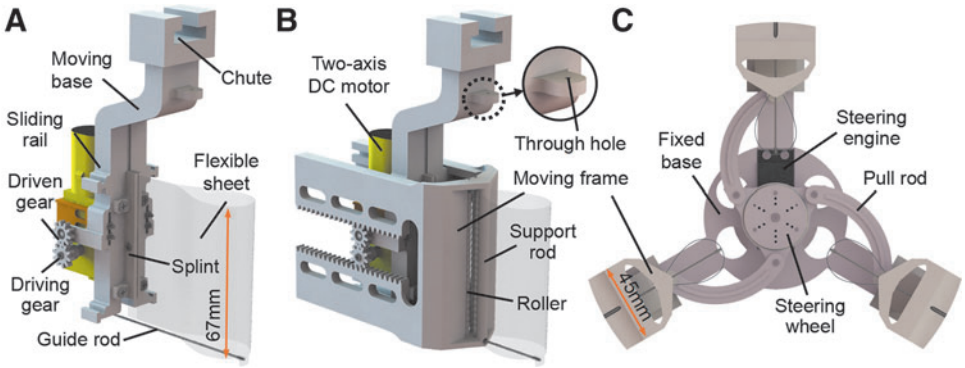

FIG. 2. Structural design of the hybrid gripper. **(A)** Structure of the hybrid gripper's finger without moving frame. **(B)** Structure of the hybrid gripper's finger with moving frame. **(C)** Upward view of the hybrid gripper.

Figure S6, the gray area available for the support rod design is constrained by the contours of the largest and smallest teardrop-shaped flexible sheets. A smaller support rod diameter means lower structural strength, but a wider range of teardrop-shaped sheet perimeter can be obtained that is directly related to the adjustable range of the finger's contact stiffness in Mode 1.

To select a suitable support rod diameter, we measured and calculated the corresponding perimeter range of support rods with different diameters based on the simulation results of the teardrop-shaped sheet contours (the simulation process is given in Section S5 of the Supplementary Data and Supplementary Figures S10–S12), and checked the strength of support rods with different diameters to calculate their maximum bearable press forces (the detailed strength check process is given in Section S4 of the Supplementary Data and Supplementary Figure S7).

Based on the above calculation results shown in Supplementary Figure S8, we finally selected 5 mm as the diameter of the support rod, and the corresponding minimum and maximum perimeters of the teardrop-shaped flexible sheet are 30 and 150 mm, respectively, since the perimeter range is relatively large under this parameter, and the maximum bearable force is also sufficient for the potential tasks of the gripper. It should be noted that 5 mm is only a relatively good result selected based on the current fabrication materials and structural parameters of the support rod, and it can be further optimized in the future.

All rigid parts of the gripper are made by a light-curing 3D printer (UNION 3D Lite600) using WEILAI 8000 resin (materials with higher performance can be chosen if necessary). The flexible sheets used here are made of polyethylene terephthalate (PET). Their outer surfaces are coated with elastomer materials of 10 μm such as Ecoflex 10 to further increase contact friction/surface, and a section of silicone tube for fixing the guide rod is glued on the bottom of their inner surfaces with silica gel. The detailed fabrication process is shown in Supplementary Figure S9.

In our current study, we chose PET to make the flexible sheets. A few concerns follow: (1) the relatively high elasticity modulus of PET can help the teardrop-shaped sheets generate obvious press force on objects when contacting with them and endow the teardrop-shaped sheets with good shape-setting ability under different gravity directions, as shown in Supplementary Movie S2; (2) the PET sheet is flexible but poor in stretchability, which ensures the stability of the teardrop-shaped sheet's perimeter and thus its contact stiffness; (3) PET sheets with various thicknesses are easily and cheaply available commercially.

This will avoid the dimensional errors that might be caused during the manual casting process and simplify the gripper's fabrication process. In addition, it should be noted that PET is not the only choice for making such teardrop-shaped sheets, other materials with similar properties, such as polyimide and polyvinyl chloride, can also be used as alternative materials.

Results

Contact stiffness in Mode 1

To verify the theoretical cubic relationships described above, we first studied the finger's contact stiffness under different geometric parameters in Mode 1 by experiment and simulation (the detailed simulation process is given in Section S5 of the Supplementary Data and Supplementary Figures S10–S12). During the tests, the finger was fed at a speed of 1 mm/s to gradually press against the test plate with its outer teardrop-shaped flexible sheet, whereas the changes of the finger's output force were recorded by a force gauge (the test setup is given in Supplementary Fig. S13).

We calculated the finger contact stiffness by linearly fitting the first third of the force versus displacement curves, which are much more common and important than the last two-third. This is because the slopes of the curves change slightly with the displacement, and calculating the contact stiffness by locally fitting the first one-third of the curves can make the calculation results closer to actual values. Similar local fitting methods have also been used in several other studies to calculate the stiffness of soft fingers.[25,26,30] In addition, the elastomer coating was proved to have no significant effect on the contact stiffness of the teardrop-shaped sheet, as shown in Supplementary Figure S14.

As shown in Figure 3A–C, the experimental curves fit well with the simulation curves, which indicates that the mechanical behaviors of the teardrop-shaped flexible sheet can be well predicted. The contact stiffness of the finger (the slopes calculated from the first one-third of the force vs. displacement curves) increases significantly with the increase of the sheet thickness and the decrease of the sheet perimeter, and there is an approximate cubic relationship between them, which agrees well with the theoretical model.

In addition, by regulating the two geometric parameters of the flexible sheet, the contact stiffness of the finger can get a maximum of 11.82 N/mm (thickness = 0.2 mm, perimeter = 30 mm) and a minimum of 0.00029 N/mm (thickness = 0.025 mm, perimeter = 150 mm), as shown in Figure 3D. Its actual stiffness adjustable range can reach considerable 40,765 times (the theoretical adjustable range is 64,000 times). The relatively large deviation between the simulation curve and the experimental curve of the maximum stiffness might be due to the plastic deformation of the PET-made flexible sheet under high pressure during the compression process.

In addition, to better reflect the contact stiffness characteristics of the teardrop-shaped flexible sheets, we also fitted the latter two-third of the curves in Figure 3A and B and calculated the corresponding contact stiffness. As shown in Supplementary Figure S15, the fitting results indicate that the contact stiffness calculated from the first one-third of the curves is generally larger than that calculated from the last two-third of the curves, with a maximum difference of $\sim$40%.

In the current design, the sheet thickness cannot be *in situ* adjusted during the gripper operation process. Thus, we investigated the adjustable range of finger contact stiffness that can be achieved by only adjusting the sheet perimeter. As shown in Supplementary Figure S16, by controlling the position of the moving frame to *in situ* adjust the perimeter of the teardrop-shaped flexible sheet, a 124 times contact stiffness adjustable range (theoretical adjustable range is 125 times) can be obtained. Moreover, the contact stiffness adjustment mechanism based on such a teardrop-shaped flexible sheet also has a series of unique advantages, such as continuous and accurate adjustable stiffness, high adjustment efficiency, and no need to introduce additional actuation principles.

We then evaluated the influence of contact surface position, size, and shape on finger contact stiffness (Fig. 3E and 3F). We found that the finger contact stiffness is inversely

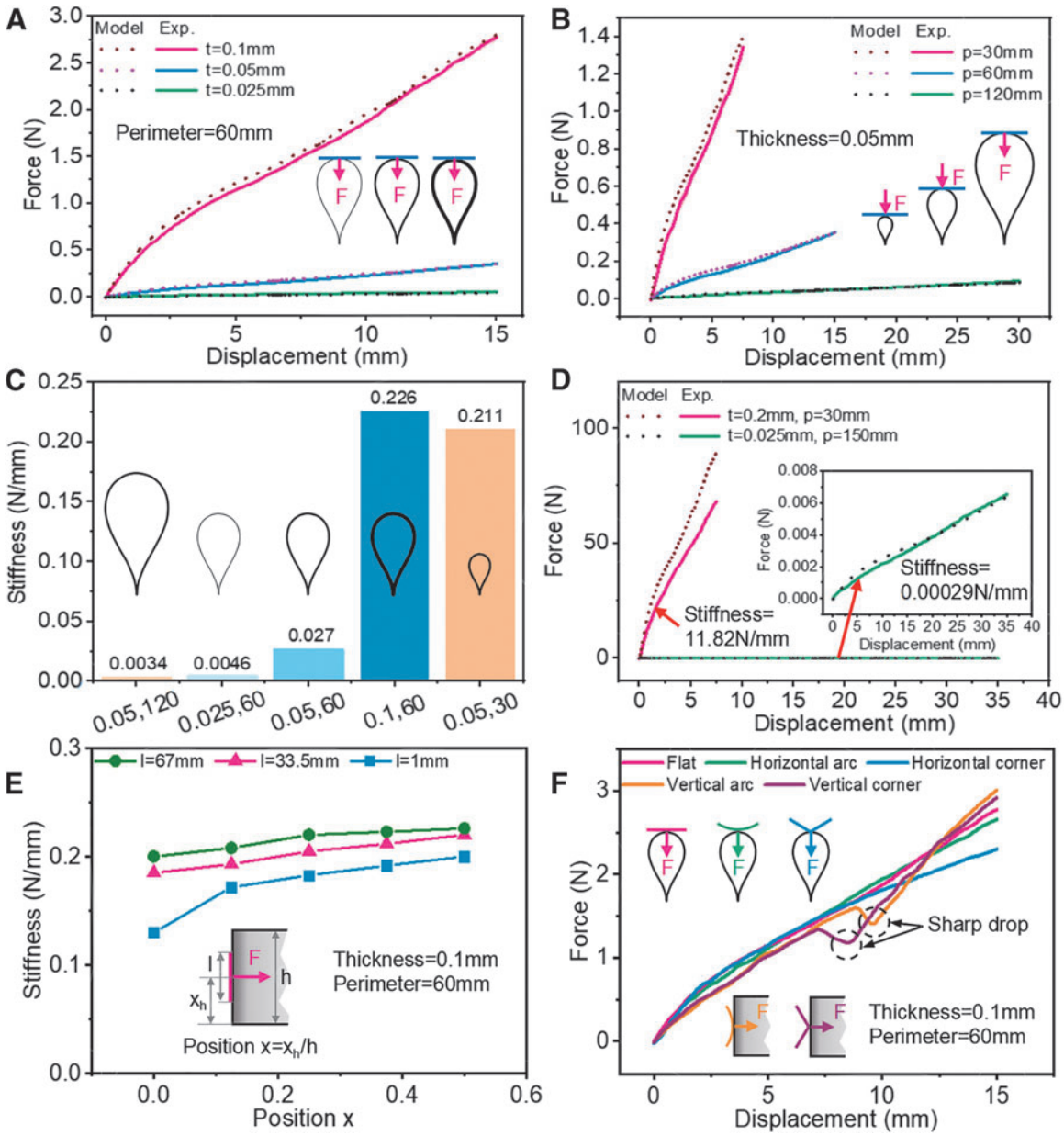

FIG. 3. Contact stiffness tests of the hybrid finger in Mode 1. **(A)** Displacement versus output force of the finger with different sheet thicknesses in Mode 1. **(B)** Displacement versus output force of the finger with different sheet perimeters in Mode 1. **(C)** Comparison of contact stiffness of the finger with different sheet thicknesses and perimeters. **(D)** Displacement versus output force of the finger with maximum and minimum contact stiffness in Mode 1. **(E)** Contact position of contact surfaces with different heights versus contact stiffness of the finger in Mode 1. **(F)** Displacement versus output force of the finger in Mode 1 when contact surfaces have different shapes.

proportional to the vertical offset of the contact surface, and directly proportional to the contact surface size. The stiffness variations might be due to the uneven deformation of the teardrop-shaped flexible sheet during its conformal process.

In addition, Figure 3F shows that the contact surface shape has relatively little influence on the finger contact stiffness (the three test plates with different surface shapes used in the experiments are shown in Supplementary Fig. S17). The sharp drops of the force versus displacement curves when the contact surface shape is in a vertical arc or corner should be caused by the plastic bending of the teardrop-shaped flexible sheet when its vertical uneven deformation is too large.

Contact compliance in Mode 1

Excellent compliance is another key feature of this finger, as its outer teardrop-shaped flexible sheet will deform compliantly and generate a large conformal area upon contacting with the objects, which will facilitate the distribution of pressure and, therefore, protect fragile objects. To demonstrate the compliance of this finger in Mode 1, simulation (the detailed

simulation process is given in Section S5 of the Supplementary Data and Supplementary Figures S10–S12) and experiments were performed to study the conformal area and pressure distribution effect of the teardrop-shaped PET sheet during the compression process, and an arched PET sheet, a solid PET fingertip, and a soft fingertip made by Ecoflex 10 (the softest material among commonly used materials in soft robots) were selected as a reference.

All three reference fingertips have the same profile as the first half of the teardrop-shaped sheet, as shown in Supplementary Figure S18. The controlled variable of the first two fingertips is the fingertip structure, whereas that of the Ecoflex 10-made soft fingertip can be viewed as the fingertip design method for achieving excellent compliance. Specifically, the Ecoflex 10-made soft fingertip represents a widely used material-based approach, which is used to fabricate soft

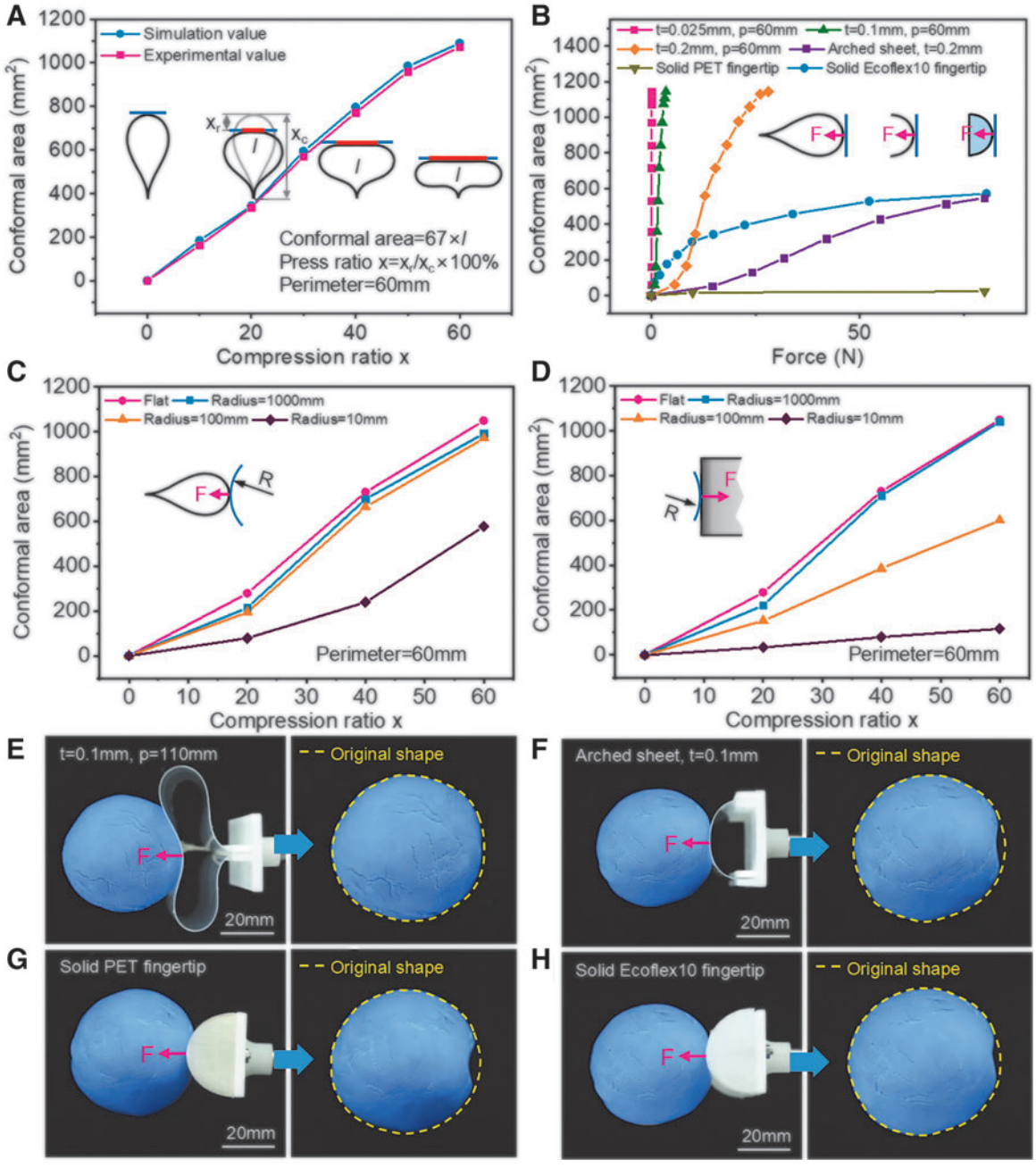

FIG. 4. Contact compliance tests of the hybrid finger in Mode 1. **(A)** Comparison of theoretical and experimental results on conformal areas of a teardrop-shaped flexible sheet under different compression ratios. **(B)** Comparison of conformal areas of three teardrop-shaped flexible sheets with different thicknesses and an Ecoflex 10 fingertip with the same profile under the same output forces. **(C)** Compression ratio versus conformal area of the teardrop-shaped flexible sheet when the contact surface has different horizontal curvatures. **(D)** Compression ratio versus conformal area of the teardrop-shaped flexible sheet when the contact surface has different vertical curvatures. **(E–H)** Compliance comparison of a teardrop-shaped PET sheet (thickness = 0.1 mm, perimeter = 110 mm), an arched PET sheet, a solid PET fingertip, and an Ecoflex 10 fingertip with the same profile under the same output force of 1 N. PET, polyethylene terephthalate.

fingertips by selecting softer materials, whereas our proposed approach is a structure-based approach, which relies on the teardrop-shaped sheet structure to achieve excellent compliance.

As shown in Figure 4A, we first compare the simulation and experimental results of the conformal areas (the conformal area is equal to the conformal length multiplied by the height of the flexible sheet when the test plate is flat) of the teardrop-shaped flexible sheet at different compression ratios. The two curves are well fitted, which proves the correctness of the simulation results. Then, we simulated and compared the conformal areas of three teardrop-shaped flexible sheets with different thicknesses with the three reference fingertips under the same output forces.

As shown in Figure 4B, the results show that the conformal areas of the teardrop-shaped flexible sheet under a certain output force increase significantly as its thickness decreases, and are significantly larger than that of the three reference fingertips, which demonstrates better compliance of the teardrop-shaped sheet structure. The reason why the conformal areas of the teardrop-shaped flexible sheet with 0.2 mm thickness is smaller than that of the Ecoflex 10-made soft fingertip in the range of 0–10 N output force might be because the relatively high contact stiffness of this teardrop-shaped flexible sheet leads to its too small compression ratio in this range.

Furthermore, we also study the influence of horizontal and vertical curvature of the contact surface on the conformal area of the teardrop-shaped flexible sheet. As shown in Figure 4C and D, the simulation results show that the conformal area is proportional to the horizontal or vertical curvature radius of the contact surface, which indicates that objects with sharp surfaces may affect the conformal effect of the teardrop-shaped flexible sheet. To better explain the results, we compare the simulation diagrams of the conformal effect of objects with different curvatures under the same compression ratio of 60%.

As shown in Supplementary Figure S19, the objects with a sharp surface will increase the conformal difficulty of the sheet, since the maximum surface curvature that can be generated by the teardrop-shaped sheet at a given compression ratio is limited. That is, it may be difficult to meet the requirement of conformal with the sharp surface.

Finally, to show the excellent compliance and pressure distribution effect of the teardrop-shaped flexible sheet more directly, we used a teardrop-shaped flexible sheet with 0.1 mm thickness and 110 mm perimeter and the three reference fingertips with the same external profile to press a fragile plasticine with a same output force of 1 N. As shown in Figure 4E–H and Supplementary Movie S3, the indentations left by the three reference fingertips are significantly more obvious than that left by the teardrop-shaped flexible sheet. The better pressure distribution effect of the teardrop-shaped flexible sheet can well protect the soft plasticine and make its surface almost leave no significant plastic deformation.

Grasping performance

The wide adjustable contact stiffness range and the excellent compliance of the fingers in Mode 1 allow them to achieve stiffness matching and compliant contact with diverse fragile objects, such as ashes, thus greatly enhancing the gripper's grasping adaptability and capability of safely grasping lightweight and fragile objects, whereas the complementary rigid mode, Mode 2 of the fingers, can further expand the gripper's capability of grasping heavy and rigid objects. To demonstrate these, we used this gripper to grasp some representative objects with various attributes. Each grasping involves a complete pick-up-and-drop-down process with at least several seconds of stable holding time.

The first explored performance is the grasping adaptability of our gripper. As shown in Figure 5 and Supplementary Movie S4, the gripper was used to grasp a series of fragile strawberries with different sizes, offsets, and poses under the same set of grasping parameters (thickness = 0.05 mm; perimeter = 70 mm; feed distance = 40 mm). The grasping results exhibit that without adjusting its working parameters, our gripper can safely grasp a set of strawberries with a maximum size difference of $\sim$18 mm ($\sim$52% of the size of the smallest strawberry), a strawberry with a left/right offset of 3 cm, and a strawberry in two different lying poses.

These results indicate that our gripper has excellent grasping adaptability, which can greatly simplify the control process and improve the grasping success rate and work efficiency of the gripper in real grasping scenes. In addition, the grasping adaptability of the gripper also has a positive correlation with the perimeter of the teardrop-shaped flexible sheet. To reflect this, the gripper was used to grasp a paper crane and plate metals, respectively, by adjusting the moving frame under the same sheet thickness as grasping strawberries (thickness = 0.05 mm).

As shown in Supplementary Movie S5, when the perimeter of the teardrop-shaped flexible sheet is 110 mm, the gripper can pick up a paper crane with an offset of up to 40 mm, whereas when the gripper is in Mode 2 (the support rod is against the teardrop-shaped flexible sheet at this moment), the gripper shows little grasping adaptability during the process of grasping the plate metals.

Wide graspable object range is another important feature of our gripper. As shown in Figure 6A and Supplementary Movie S6, a gripper with 0.025 mm thick flexible sheets can reach a very low contact stiffness and thus can easily pick up a piece of cigarette ash and incense ash without any obvious damage, which is quite difficult for human hands and almost all existing soft/hybrid grippers. Such a gripper can also well grasp some other lightweight and fragile objects such as a piece of potato chip, an origami paper crane, a strawberry, or even a living fish in Mode 1 by adjusting the thickness and perimeter of its teardrop-shaped flexible sheets.

Moreover, as shown in Figure 6B, when the gripper is switched to Mode 2, it can stably lift a series of heavy and rigid objects such as 3.2 kg plate metals and a 5.1 kg dumbbell. By strengthening its rigid structures or selecting more powerful steering engines, the load capacity of the gripper can be further expanded.

In addition, as shown in Supplementary Movie S7, by online adjusting its contact stiffness, the gripper can continuously grasp a series of objects with diverse degrees of fragility, which indicates that the gripper can still have a relatively wide range of graspable objects when its sheet thickness is constant.

We also evaluated the lateral grasping ability of the gripper. As shown in Supplementary Movie S8, our gripper is capable of grasping a range of objects from the side, such as a suspended cherry. The good shape-setting ability of the teardrop-shaped sheets mentioned above under different gravity directions makes the contact stiffness characteristics of the gripper still effective in the lateral grasping process. In addition, for better lateral

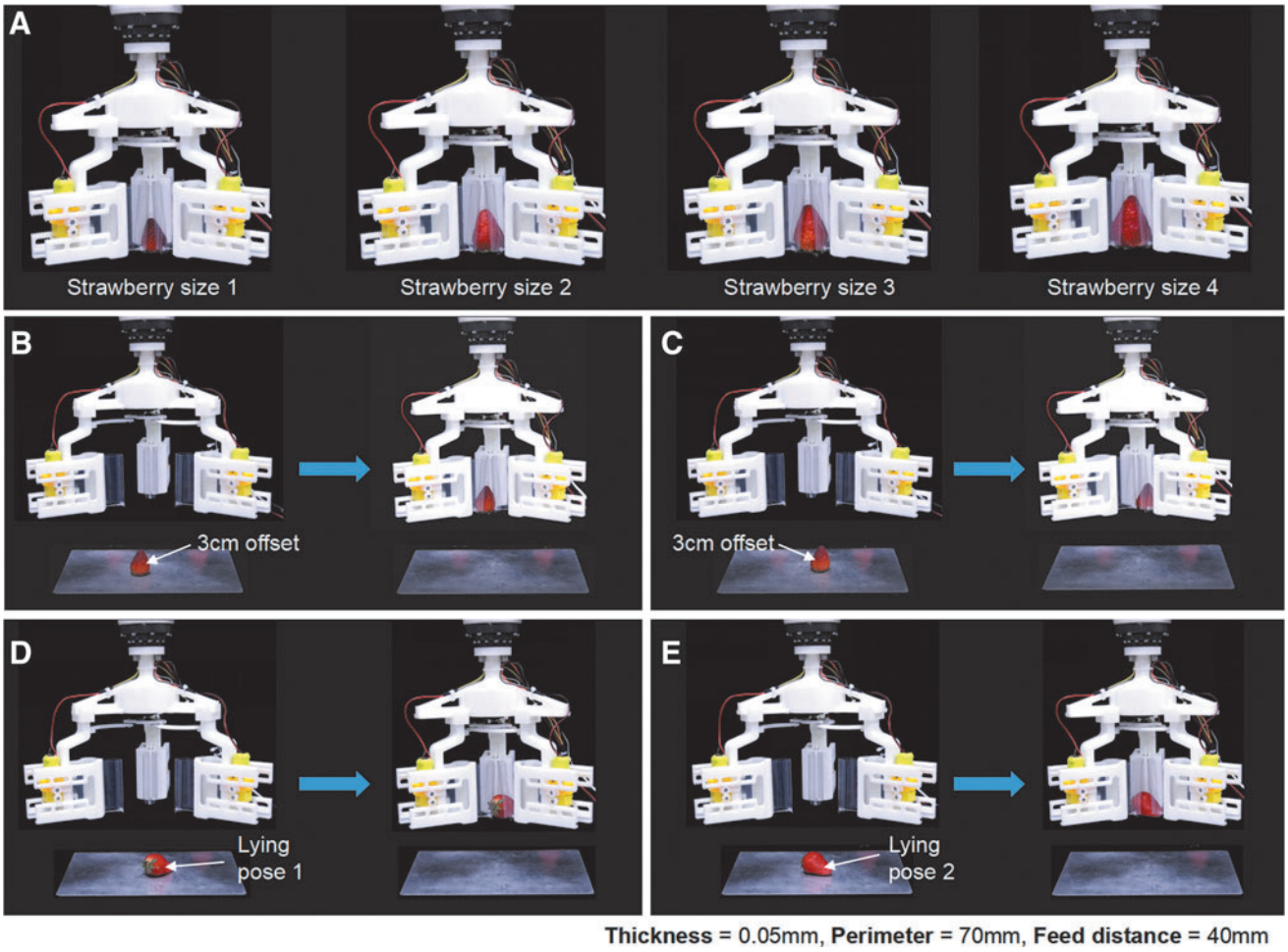

FIG. 5. High grasping adaptability of the hybrid gripper. The gripper working parameters during the tests were determined: sheet thickness = 0.05 mm, sheet perimeter = 70 mm, and feed distance = 40 mm. **(A)** The hybrid gripper can grasp a set of strawberries with different sizes (strawberry size 1: 30 × 30 × 38 mm; strawberry size 2: 35 × 35 × 45 mm; strawberry size 3: 40 × 40 × 50 mm; strawberry size 4: 47 × 47 × 57 mm). **(B)** The hybrid gripper can grasp a strawberry with a left offset of 3 cm. **(C)** The hybrid gripper can grasp a strawberry with a right offset of 3 cm. **(D)** The hybrid gripper can grasp a strawberry in lying pose 1. **(E)** The hybrid gripper can grasp a strawberry in lying pose 2.

grasping, we also designed a two-fingered gripper configuration that can be fabricated in the future for grasping various objects placed on the table, such as cups and fruits, from the horizontal direction, as shown in Supplementary Figure S20.

Conclusion and Discussion

In summary, we developed a dual-modal hybrid gripper with three hybrid fingers. Its two modes switched by controlling the position of the fingers' moving frames can selectively highlight the low contact stiffness and excellent compliance of the teardrop-shaped flexible sheets and the high contact stiffness of the moving frames. Moreover, the contact stiffness of the teardrop-shaped sheet can be wide-range adjusted by online controlling the moving frame position or offline replacing sheets with different thicknesses. The compliance of the teardrop-shaped flexible sheet also proved to be excellent compared with an Ecoflex 10 fingertip with the same profile.

Such a hybrid gripper with a wide tunable contact stiffness range and high compliance shows excellent grasping adaptability (can safely grasp a set of fragile strawberries with a maximum size difference of ∼18 mm, a strawberry with a left/right offset of 3 cm, and a strawberry in two different lying poses) and wide graspable object range (from 0.1 g super fragile cigarette ash to a 5.1 kg dumbbell).

Contact stiffness, reflecting the force characteristics of robotic grippers during interaction processes, directly affects their capability of manipulating fragile objects. To obtain a wider graspable object range, numerous researchers have tried to use soft materials to fabricate robotic grippers to obtain a relatively low contact stiffness, and further introduced multiple variable stiffness mechanisms to enhance their load capacity. However, the variable stiffness components, such as granular cavities, will inevitably limit the lower limit of contact stiffness that can be achieved by these soft grippers, and the improved loading capacities are still quite limited.

Our gripper design demonstrates another feasible or even better way to ensure high loading capacity while obtaining sufficiently low contact stiffness, which is obtained by introducing soft/compliant structures with the capability of achieving extremely low contact stiffness above the contact surface of grippers with high structural stiffness.

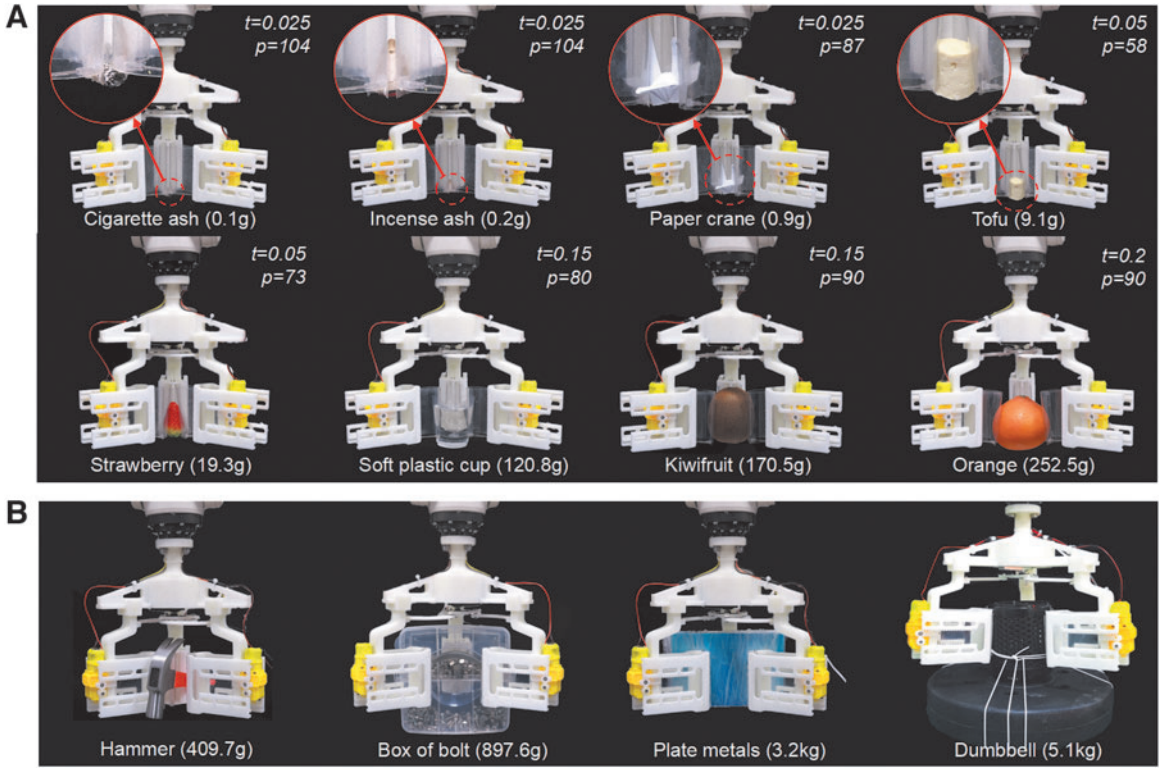

FIG. 6. Wide graspable objects range of the hybrid gripper. The *t* means thickness and the *p* means perimeter. **(A)** The hybrid gripper can grasp a wide range of fragile and lightweight objects in Mode 1. The first line from *left* to *right*: cigarette ash (0.1 g), incense ash (0.2 g), a paper crane (0.9 g), and a piece of tofu (9.1 g). The second line from *left* to *right*: a strawberry (19.3 g), a soft plastic cup (120.8 g), a kiwifruit (170.5 g), and an orange (252.5 g). **(B)** The hybrid gripper can grasp a wide range of heavy and rigid objects in Mode 2 such as a hammer (409.7 g), box of bolts (897.6 g), plate metals (3.2 kg), and dumbbells (5.1 kg).

Moreover, the teardrop-shaped flexible sheets made of PET demonstrate a promising structure-based way to integrate excellent compliance and wide tunable contact stiffness range in a compact robotic system, which is difficult to achieve with traditional material-based ways (i.e., selecting softer fabrication materials). This reflects the great potential of compliant structures in improving robot performance. By introducing such compliant structures with unique mechanical properties into robotic systems, some other attractive possibilities might also be enabled, such as computing, energy storage, and mode switching.

This study can serve as a reference for subsequent research on high-performance robot development, and the gripper has the potential to be used in various fields such as human–robot interaction, industrial sorting, biological sample collection, and food processing. Furthermore, by integrating control chips, our gripper is expected to be an untethered Bluetooth-controlled system, which has excellent portability.

Authors' Contributions

J.Z. and H.C. contributed equally to this study. J.Z. conceived and initiated the concept, built the theoretical models, designed the experiments, and drafted the article. J.Z. and H.C. designed and iterated the prototypes, and carried out the experiments and data processing. J.Z., H.C., and Z.C. performed the simulations. Z.W. directed the research and edited the article. All authors contributed to the discussion.

Author Disclosure Statement

No competing financial interests exist.

Funding Information

The materials based on the study are partly financially supported by the National Natural Science Foundation of China (Grant Nos. 52188102 and U1613204).

Supplementary Material

Supplementary Data S1
Supplementary Movie S1
Supplementary Movie S2
Supplementary Movie S3
Supplementary Movie S4
Supplementary Movie S5
Supplementary Movie S6
Supplementary Movie S7
Supplementary Movie S8
Supplementary Figure S1
Supplementary Figure S2
Supplementary Figure S3
Supplementary Figure S4
Supplementary Figure S5
Supplementary Figure S6
Supplementary Figure S7
Supplementary Figure S8

Supplementary Figure S9
Supplementary Figure S10
Supplementary Figure S11
Supplementary Figure S12
Supplementary Figure S13
Supplementary Figure S14
Supplementary Figure S15
Supplementary Figure S16
Supplementary Figure S17
Supplementary Figure S18
Supplementary Figure S19
Supplementary Figure S20

References

1. Liu W, Duo Y, Liu J, et al. Touchless interactive teaching of soft robots through flexible bimodal sensory interfaces. Nat Commun 2022;13:5030.
2. Lin Y, Zhang C, Tang W, et al. A bioinspired stress-response strategy for high-speed soft grippers. Adv Sci 2021;8:2102539.
3. Gu G, Zhang N, Xu H, et al. A soft neuroprosthetic hand providing simultaneous myoelectric control and tactile feedback. Nat Biomed Eng 2023;7:589–598.
4. Zhang Y, Zhang W, Gao P, et al. Finger-palm synergistic soft gripper for dynamic capture via energy harvesting and dissipation. Nat Commun 2022;13:7700.
5. Galloway KC, Becker KP, Phillips B, et al. Soft robotic grippers for biological sampling on deep reefs. Soft Robot 2016;3:23.
6. Tessler M, Brugler MR, Burns JA, et al. Ultra-gentle soft robotic fingers induce minimal transcriptomic response in a fragile marine animal. Curr Biol 2020;30:157–158.
7. Wang Z, Kanegae R, Hirai S. Circular shell gripper for handling food products. Soft Robot 2021;8:542–554.
8. Kuriyama Y, Okino Y, Wang Z, et al. A wrapping gripper for packaging chopped and granular food materials. In: IEEE International Conference on Soft Robotics (RoboSoft). IEEE: Seoul, Korea (South); 2019; pp. 114–119.
9. Lee JY, Seo YS, Park C, et al. Shape-adaptive universal soft parallel gripper for delicate grasping using a stiffness-variable composite structure. IEEE Trans Ind Electron 2020;68:12441–12451.
10. Hao Y, Gong Z, Xie Z, et al. Universal soft pneumatic robotic gripper with variable effective length. In: Chinese Control Conference (CCC). IEEE: Chengdu, China; 2016; pp. 6109–6114.
11. Rodriguez A. The unstable queen: Uncertainty, mechanics, and tactile feedback. Sci Robot 2021;6:eabi4667.
12. Laffranchi M, Boccardo N, Traverso S, et al. The Hannes hand prosthesis replicates the key biological properties of the human hand. Sci Robot 2020;5:eabb0467.
13. Xiong CH, Chen WR, Sun BY, et al. Design and implementation of an anthropomorphic hand for replicating human grasping functions. IEEE Trans Robot 2016;32:652–671.
14. Hang K, Bircher WG, Morgan AS, et al. Manipulation for self-Identification, and self-Identification for better manipulation. Sci Robot 2021;6:eabe1321.
15. Yan Y, Hu Z, Yang Z, et al. Soft magnetic skin for super-resolution tactile sensing with force self-decoupling. Sci Robot 2021;6:eabc8801.
16. Becker K, Teeple C, Charles N, et al. Active entanglement enables stochastic, topological grasping. Proc Natl Acad Sci U S A 2022;119:e2209819119.
17. Hong Y, Chi Y, Wu S, et al. Boundary curvature guided programmable shape-morphing kirigami sheets. Nat Commun 2022;13:530.
18. Liu X, Zhao Y, Geng D, et al. Soft humanoid hands with large grasping force enabled by flexible hybrid pneumatic actuators. Soft Robot 2021;8:175–185.
19. Zhang YF, Zhang N, Hingorani H, et al. Fast-response, stiffness-tunable soft actuator by hybrid multimaterial 3D printing. Adv Funct Mater 2019;29:1806698.
20. Yang Y, Vella K, Holmes DP. Grasping with kirigami shells. Sci Robot 2021;6:eabd6426.
21. Abondance S, Teeple CB, Wood RJ. A dexterous soft robotic hand for delicate in-hand manipulation. IEEE Robot Autom Lett 2020;5:5502–5509.
22. Li H, Yao J, Liu C, et al. A bioinspired soft swallowing robot based on compliant guiding structure. Soft Robot 2020;7:491–499.
23. Xie Z, Domel AG, An N, et al. Octopus arm-inspired tapered soft actuators with suckers for improved grasping. Soft Robot 2020;7:639–648.
24. Zhou J, Chen Y, Hu Y, et al. Adaptive variable stiffness particle phalange for robust and durable robotic grasping. Soft Robot 2020;7:743–757.
25. Yang Y, Zhang Y, Kan Z, et al. Hybrid jamming for bioinspired soft robotic fingers. Soft Robot 2020;7(3):292–308.
26. Wei Y, Chen Y, Ren T, et al. A novel, variable stiffness robotic gripper based on integrated soft actuating and particle jamming. Soft Robot 2016, 3(3): 134–143.
27. Brown E, Rodenberg N, Amend J, et al. Universal robotic gripper based on the jamming of granular material. Proc Natl Acad Sci U S A 2010;107:18809–18814.
28. Li Y, Chen Y, Yang Y, et al. Passive particle jamming and its stiffening of soft robotic grippers. IEEE Trans Robot 2017;33:446–455.
29. Shintake J, Schubert B, Rosset S, et al. Variable stiffness actuator for soft robotics using dielectric elastomer and low-melting-point alloy. In: IEEE/RSJ International Conference on Intelligent Robots and Systems (IROS). IEEE: Hamburg, Germany; 2015; pp. 1097–1102.
30. Yang Y, Chen Y, Li Y, et al. Novel variable-stiffness robotic fingers with built-in position feedback. Soft Robot 2017;4:338–352.
31. Linghu C, Zhang S, Wang C, et al. Universal SMP gripper with massive and selective capabilities for multiscaled, arbitrarily shaped objects. Sci Adv 2020;6:eaay5120.
32. Firouzeh A, Paik J. Grasp mode and compliance control of an underactuated origami gripper using adjustable stiffness joints. IEEE/ASME Trans Mech 2017;22:2165–2173.
33. Xing Z, McCoul D, Wang F, et al. Principle of stiffness variation based on matching composite structures with fibers. Smart Mater Struct 2020;29:095017.
34. Dong X, Tang C, Jiang S, et al. Increasing the payload and terrain adaptivity of an untethered crawling robot via soft-rigid coupled linear actuators. IEEE Robot Autom Lett 2021;6:2405–2412.
35. Fu HC, Ho JDL, Lee KH, et al. Interfacing soft and hard: A spring reinforced actuator. Soft Robot 2020;7:44–58.
36. Qin L, Liang X, Huang H, et al. A versatile soft crawling robot with rapid locomotion. Soft Robot 2019;6:455–467.
37. Li Y, Ren T, Li Y, et al. Untethered-bioinspired quadrupedal robot based on double-chamber pre-charged pneumatic soft actuators with highly flexible trunk. Soft Robot 2021;8:97–108.

38. Dong X, Wang Y, Liu XJ, et al. Development of modular multi-degree-of-freedom hybrid joints and robotic flexible legs via fluidic elastomer actuators. Smart Mater Struct 2022;31:035034.
39. Zhu J, Chai Z, Yong H, et al. Bioinspired multimodal multipose hybrid fingers for wide-range force, compliant, and stable grasping. Soft Robot 2023;10:30–39.
40. Shen Z, Zhong H, Xu E, et al. An underwater robotic manipulator with soft bladders and compact depth-independent actuation. Soft Robot 2020;7:535–549.
41. Tang Y, Chi Y, Sun J, et al. Leveraging elastic instabilities for amplified performance: Spine-inspired high-speed and high-force soft robots. Sci Adv 2020;6:eaaz6912.
42. Zhu J, Pu M, Chen H, et al. Pneumatic and tendon actuation coupled muti-mode actuators for soft robots with broad force and speed range. Sci China Technol Sci 2022;65:2156–2169.
43. Su Y, Fang Z, Zhu W, et al. A high-payload proprioceptive hybrid robotic gripper with soft origamic actuators. IEEE Robot Autom Lett 2020;5:3003–3010.

Address correspondence to:
Zhigang Wu
Soft Intelligence Laboratory
State Key Laboratory of Digital Manufacturing Equipment and Technology
Huazhong University of Science and Technology
Wuhan 430074
China

E-mail: zgwu@hust.edu.cn